Final Report

Title:

Functionalizing Carbon Nanotubes and Related Nanostructures for Various Applications

AFOSR/AOARD Reference Number:
AOARD-07-4077

AFOSR/AOARD Program Manager:
Thomas Erstfeld

Period of Performance:
1 July 2007- 30 June 2009

Submission Date:
14 November 2009

Main PI:
Dr. Li-Chyong Chen, Research Fellow
Center for Condensed Matter Sciences, National Taiwan University
1, Roosevelt Road, Section 4, Taipei 106, Taiwan
Tel: 886-2-3366-5249; Fax: 886-2-2365-5404
E-mail:chenlc@ntu.etdu.tw

Co-PI:
Dr. Kuei-Hsien Chen, Research Fellow
Institute of Atomic and Molecular Sciences, Academia Sinica
PO Box 23-166, Taipei 106, Taiwan
Tel: 886-2-2366-8232; Fax: 886-2-2362-0200
E-mail:chenkh@pub.iams.sinica.edu.tw

Report Documentation Page

Form Approved
OMB No. 0704-0188

1. REPORT DATE **17 DEC 2009**	2. REPORT TYPE **FInal**	3. DATES COVERED **14-06-2007 to 13-06-2029**

4. TITLE AND SUBTITLE **Functionalizing Carbon Nanotubes and Related Nanostructures for Various Applications**	5a. CONTRACT NUMBER **FA48690714077**
	5b. GRANT NUMBER
	5c. PROGRAM ELEMENT NUMBER
6. AUTHOR(S)	5d. PROJECT NUMBER
	5e. TASK NUMBER
	5f. WORK UNIT NUMBER
7. PERFORMING ORGANIZATION NAME(S) AND ADDRESS(ES) **National Taiwan University,1, Roosevelt Road. Section 4,Taipei 106,Taiwan,TW,106**	8. PERFORMING ORGANIZATION REPORT NUMBER **N/A**
9. SPONSORING/MONITORING AGENCY NAME(S) AND ADDRESS(ES) **AOARD, UNIT 45002, APO, AP, 96337-5002**	10. SPONSOR/MONITOR’S ACRONYM(S) **AOARD**
	11. SPONSOR/MONITOR’S REPORT NUMBER(S) **AOARD-074077**

12. DISTRIBUTION/AVAILABILITY STATEMENT

Approved for public release; distribution unlimited

13. SUPPLEMENTARY NOTES

14. ABSTRACT

This report deals with highly functionalized devices involving multi-components and heterogeneous interfaces for which nano-scale control is useful. The researcher then describes six different types of devices.

15. SUBJECT TERMS

Nano-Materials

16. SECURITY CLASSIFICATION OF:			17. LIMITATION OF ABSTRACT	18. NUMBER OF PAGES	19a. NAME OF RESPONSIBLE PERSON
a. REPORT **unclassified**	b. ABSTRACT **unclassified**	c. THIS PAGE **unclassified**	**Same as Report (SAR)**	**23**	

Standard Form 298 (Rev. 8-98)
Prescribed by ANSI Std Z39-18

Abstract

Highly functional devices usually involve multi-components and heterogeneous interfaces, of which nano-scale control is crucial. Six cases are exemplified here: (1) miniaturized micro direct-methanol-fuel-cells (DMFC) using CN_xNTs with low loading of precious metals, (2) high-performance supercapacitor with ultrafast charging-discharging property using direct growth of arrayed CN_xNT-RuO_2 nanocomposites, (3) ultrahigh photocurrent gain in m-axial GaN NWs and nanobridges, (4) biomimetic SiNTs with broadband and quasi-omni-directional anti-reflection properties, (5) methanol-tolerant membrane for DMFC based on Nafion/polyaniline nanowires, and (6) sieve-layer mediated solar cell based on ZnPc/Si *p-n* junctions. On-chip wafer processes have been applied to fabricate vertically aligned, high-density arrays of carbon nanotubes (CNTs), bridging gallium nitride nanowires (GaN NWs), arrayed silicon nanotips (SiNTs) and layered organic-inorganic hybrids. These nanomaterials and their hybrids show unique electrical, electrochemical, optical, photoconductivity and photovoltaic properties.

Introduction

A number of photonic, photovoltaic and electrochemical devices that utilize low-dimensional nanomaterials, including carbon nanotubes, semiconductor and organic (or polymeric) nanowires and thin layers, as their key components have been investigated. Composite structures of nanowires/nanoparticles and organic/inorganic hybrid materials having different functionalities were developed using a variety of process techniques, including microwave plasma enhanced chemical vapor deposition (MW-PECVD), electron-cyclotron-resonance (ECR) PECVD, ion beam sputtering, magnetron sputtering, as well as atom- and ion-beam assisted processes. All these techniques involve synthesizing materials in conditions far away from equilibrium process; therefore, they offer an unprecedented opportunity for forming metastable phases and novel structures that can not be produced by the conventional techniques.

For carbon nanotubes (CNTs), we have established a strong foundation in vertically aligned CNTs arrays [1]. Major accomplishments in the past include employing Si-based wafer techniques for fabricating CNTs-based integrated devices such as gated and TFT-controlled field emission devices. More recently, significant efforts have been devoted to the functionalization of CNTs and micro-energy device fabrication. An efficient and simple route to attach Pt and Ru nanoparticles (NPs), ca. 2 nm in average diameter, on the sidewalls of vertically aligned CNTs arrays on Si substrates has been developed [2]. We believed that nitrogen incorporation in the carbon nanotubes played a key role for high-density nucleation of ultra-fine nanoparticles [3]. Electrochemical investigation suggests Pt NPs are electronically accessible through CN_x NTs and they exhibit favorable electron transfer properties with H_2 production and methanol (CH_3OH) oxidation. The later finding is especially interesting in the context of the bipolar plates' application in the micro direct methanol fuel cell (μDMFC) devices. In fact, an "on-chip" approach, which is well established in the Si wafer-based micro-electronic industry, has been extended to carbon cloth for micro-energy devices. Our synthetic technique for producing CNTs-modified carbon cloth is highly efficient in subsequent loading of precious metal, in that we obtain a similar power performance with only one tenth of loading, in comparison to that of the conventional method, thus, enabling a significant cost-reduction in fuel cells [4-5]. Moreover, high performance supercapacitor has been demonstrated using arrayed

CN_xNT-RuO_2 nanocomposites directly grown on Ti-buffered Si substrate [6-7]. Novel engineering at each individual pair of heterogeneous interface ensures excellent current collection and charge-discharge efficiency. A record high specific capacitance of 1380 F/g-RuO_2, close to theoretical limit, a fast charging–discharging rate (up to 600 mV/s), and high operation stability (over 5000 cycles) have been obtained [8].

The nanostructure-enabled (and/or –enhanced) properties are not unique to CNTs only but also seen in a variety of semiconductors, such as GaN and Si. Based on our catalytic chemical vapor deposition for producing ensemble of nanowires, we have further demonstrated a viable nanobridge (NB) device by direct integration of an ensemble of GaN nanowires onto a microchip [9]. Ultrahigh photocurrent responsivity to the UV irradiation has been observed in the GaN NBs. The on-chip NB-based devices thus fabricated provide large surface area, short transport path, high responsivity for next generation sensors and detectors.

Among all the studies during this 2-yr project period, our work on SiNTs has attracted most attention. The SiNTs were produced by a patented ECR plasma-assisted self-mask dry-etching method. Conventional photolithography-oxidation-stripping and pulsed laser chemical etching processes can produce Si tips of microns or submicrons only. In contrast, the ECR process, with the advantage of highest density of plasma of all, offers the opportunity for fabricating forest of Si tips down to nanometer scale. This new etching technique can also be applied to a variety of materials such as GaN, GaP, metals and glass [10]. A US patent and a Taiwan patent have been awarded in 2005 [11]. The large area subwavelength structure that mimicked a moth eye demonstrated a low hemispherical reflectance of <1% from ultraviolet to the infrared region and show significant suppression of specular reflection in the far-infrared to terahertz region. The remarkably high and featureless optical absorption in the aperiodic SiNTs, as against the periodic sub wavelength structures, promises enhanced performance in solar cell applications. This particular work is published in Nature Nanotechnology [12] and also featured in March 2008 by Asia-Materials, Nature Publishing Group.

Finally, we have extended our efforts to organic or polymeric materials, more specifically, their hybrids with inorganic materials. Two cases are reported here: (i) the methanol-tolerant fuel cell membrane based on polyaniline nanowires and Nafion hybrids [13], and (ii) sieve-layer mediated solar cell based on ZnPc/Si *p-n* junctions [14].

Important research findings and their implications for future technology development or applications are summarized below.

Categorized Summary of Research Outcomes

(1) Miniaturized micro direct-methanol-fuel-cells using carbon nanotubes with low loading of precious metals

The feasibility of a high-performance membrane-electrode-assembly (MEA), with low electrocatalyst loading on CNTs grown directly on carbon cloth (CC) as an anode, is demonstrated. The direct growth of CNTs was synthesized by microwave plasma-enhanced chemical vapor deposition (MW-PECVD) using $CH_4/H_2/N_2$ as precursors. The cyclic voltammetry (CV) and electrochemical impedance measurements with $1mMFe(CN)_6^{3-/4-}$ redox reaction reveal a fast electron transport and a low resistance of charge transfer on the direct growth of CNTs. The electrocatalysts, platinum and ruthenium, were coated on CNTs by sputtering to form Pt-Ru/CNTs-CC composites. Pt-Ru electrocatalysts are uniformly dispersed on the CNTs, as indicated by high-resolution scanning electron microscopy (HRSEM) and transmission electron microscopy (TEM), because the nitrogen doped in the CNT acts as active sites for capturing electrocatalysts. The MEA, the sandwiched structure which comprises 0.4 mg cm^{-2} Pt-Ru/CNTs-CC as the anode, 3.0 mg cm^{-2} Pt black as the cathode and Nafion 117 membrane at the center, performs very well in a DMFC test. The micro-structural MEA analysis shows that the thin electrocatalyst layer is uniform, with good interfacial continuity between membrane and the gas diffusion layer. Figure 1 presents CV measurements for the Pt-Ru/CNTs-CC and the Pt-Ru/CC in 1M methanol solution and 1M sulfuric acid at a scan rate of $10mVs^{-1}$. At a given metal loading of 0.4 mg cm^{-2}, the onset potential of the methanol oxidation of the Pt-Ru/CNTs-CC is lower than that of the Pt-Ru/CC in the anodic sweep, which indicates that the Pt-Ru/CNTs-CC indeed reduces the activation overpotential. Furthermore, the improvement in performance associated with the use of a CNTs-CC composite anode in DMFC can be clearly seen in the polarization curves of the cells

(Figure 2). Much higher maximum power density can be obtained even with an order-of-magnitude smaller loading of precious metal.

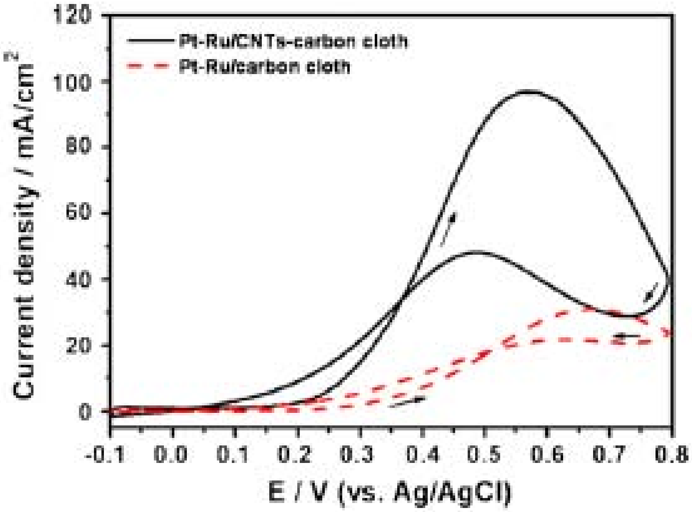

Figure 1 Comparative CV measurements for Pt-Ru on CNTs-carbon cloth electrode and plain carbon cloth in 1M methanol/1M sulfuric acid solution operated at room temperature and a scan rate of $10 mVs^{-1}$.

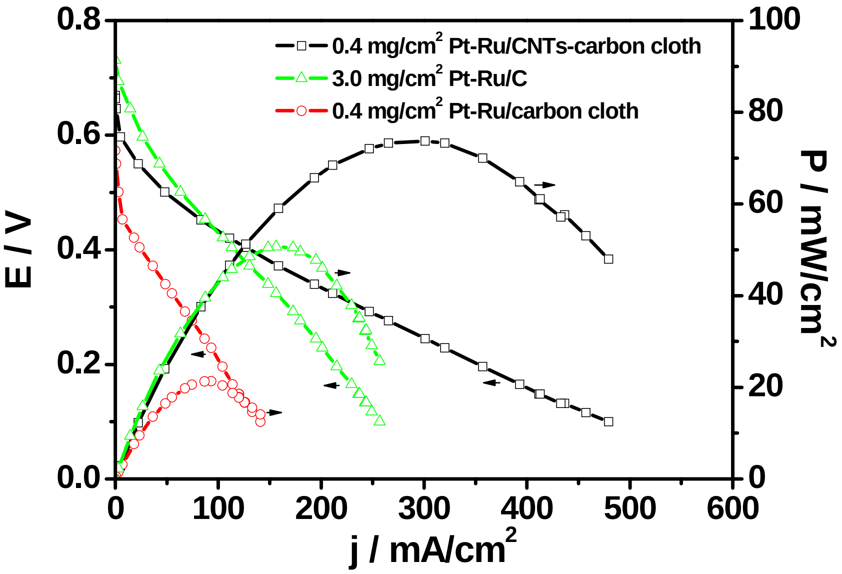

Figure 2 Polarization curves of DMFCs using various anodes operated at 60 ˚C with 1M methanol and oxygen feeding to anode and cathode, respectively.

(2) High-performance supercapacitor with ultrafast charging-discharging property using direct growth of CN_xNT-RuO_2 nanocomposites arrays

Significant enhancement in supercapacitor performance has been achieved via a new RuO_2 nanocomposite materials prepared by direct ruthenium sputtering on arrayed multiwalled carbon nanotubes supported by Ti-buffered Si wafer. X-ray photoelectron spectroscopy, HRTEM and selective area electron diffraction analyses reveal that the as-prepared nanoparticles (NPs) have a crystalline Ru metal core with RuO_2 oxide coating. The nanocomposites convert to RuO_2–CN_x NTs with subsequent electrochemical cycling, leading to well-dispersed and strongly adhered RuO_2 NPs densely populated on CN_x NTs (Figure 3). The arrayed CN_xNT-RuO_2 nanocomposites so-obtained exhibit an outstanding capacitance property, with an overall specific capacitance of 1380 F/g-RuO_2, close to theoretical limit, a fast charging–discharging rate (up to 600 mV/s), and high operation stability (over 5000 cycles), as shown in Figure 4. Thus, RuO_2–CN_x NTs nanocomposites would make a promising candidate for use in next-generation high efficiency miniaturized supercapacitors directly fabricated on Si substrate.

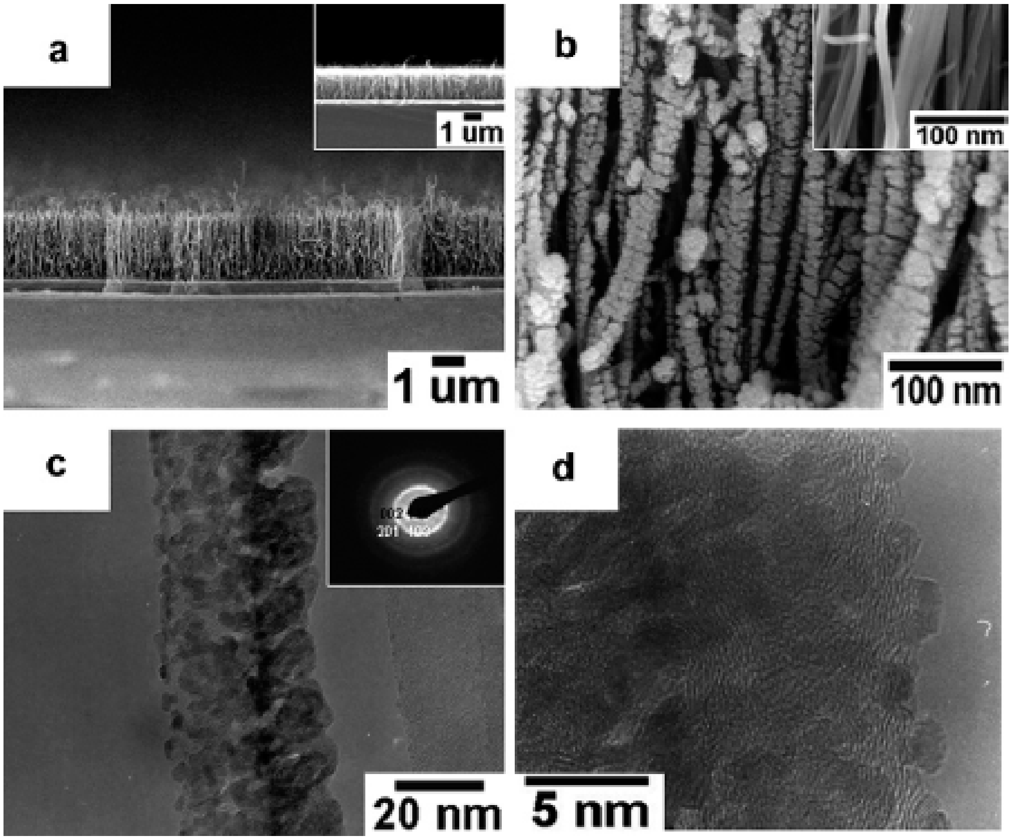

Figure 3 (a) Low-magnification and (b) high-magnification cross-sectional HRSEM images of arrayed nanocomposites grown on Ti-buffered Si substrates. The insets show as-grown NTs prepared by MPECVD. (c) Low-magnification TEM and (d) HRTEM images of a single CNx NT with Ru/RuO2 coating. The insets in (c) display the corresponding SAED pattern and histogram of NPs on the NT sidewalls. The sputtering deposition condition of 140 W for 20 min is used.

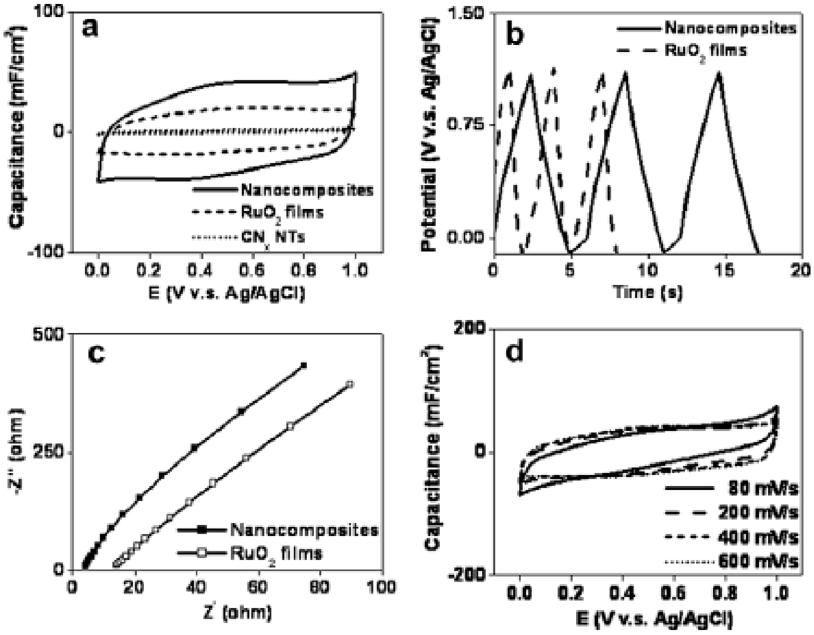

Figure 4 (a) Comparison of capacitance– voltage curves of CN_x NTs, RuO_2 films and nanocomposites at the scan rate of 600 mV/s, (b) corresponding charging–discharging curves of RuO_2 films and nanocomposites at constant current density of 23 mA/cm^2, (c) corresponding frequency response of films and nanocomposites at 0.8 V (freq. = 0.01– 104 Hz) and (d) scan rate dependent capacitance of nanocomposites from 80 to 600 mV/s. A sputtering deposition condition of 140 W for 20 min is used. (Electrolyte = 1 M H_2SO_4).

(3) Ultrahigh photocurrent gain in m-axial GaN nanowires

Group III nitrides form an important class of optoelectronic materials with capability of full-color applications, i.e., in optical wavelength ranging from IR to UV. The low dimensional nanostructures often exhibit novel electronic and optoelectronic properties unmatched by their bulk or thin film counterparts. For instance, InN nanobelts showed photoluminescence in IR with a peak width of 14 meV, the sharpest reported to date for InN [15]. The rectangular cross-sectional nanobelt has the potential to serve as an effective Fabry-Perot microcavity for lasing process [16]. Unlike the “epitaxial” film, wherein lattice mismatch between the film and the substrate often gives rise to very high density of extended defects, these free-standing nanostructures are nearly defect-free, as exemplified by weak temperature quenching in the photoluminescence property of InN nanotips, implying high quantum efficiency. Interestingly, contrary to the quantum confinement effect commonly believed to occur at a particle size or wire diameter below Bohr radius, we have observed anomalous blue shift in the III-N and ZnO nanowires, with diameters far beyond the quantum confinement regime. Strong surface effect was suggested for this behavior as well as its induced piezoelectricity and photoelastic effects in the case of InN nanobelts [17].

More recently, an on-chip fabrication of an ensemble of aligned and contact barrier-free GaN nanobridges for device application is demonstrated [9]. The device architecture is shown in Figure 5, wherein a design of heavily doped and homogeneous semiconducting layer as contact buffer enables self-formed ohmic contacts between the GaN nanobridges and metal electrode and at the same time, assists the growth alignment of these one-dimensional nanostructures. The GaN nanobridge devices exhibit an excellent visible-blind performance for the UV light detection. The ultrahigh photocurrent generation efficiency is also found from these bridging GaN nanowires, consistent with single-wire measurements. As depicted in Figure 6, with decreasing wire diameter, ultrahigh responsivity ($R > 10^6$ A/W) and gain ($\Gamma > 10^7$) in photoconduction are observed in GaN nanowires, several orders of magnitude higher than their thin film counterparts [18].

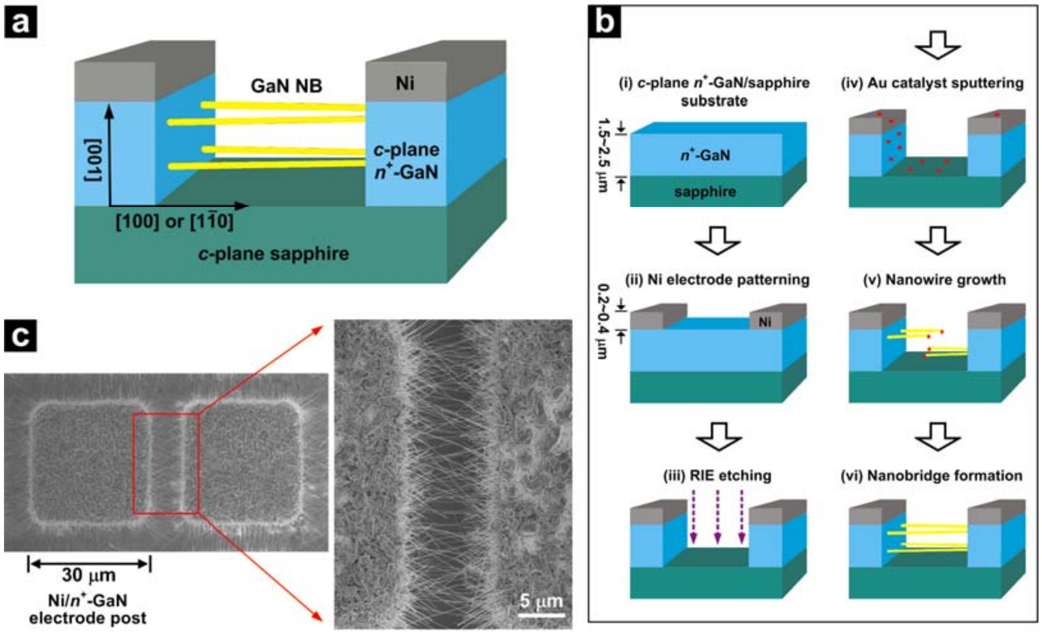

Figure 5 a) The schematic architecture of the GaN nanobridge device. The arrows indicate the *c*-plane n^+-GaN electrode posts with [100] and [$1\bar{1}0$] side walls. b) The schematic fabrication process of the GaN nanobridge device. c) Top-view FESEM

images of a GaN nanobridge device focused on one pair of Ni/*n*$^+$-GaN electrode post (left) and on the trench with nanowires bridging between two posts (right).

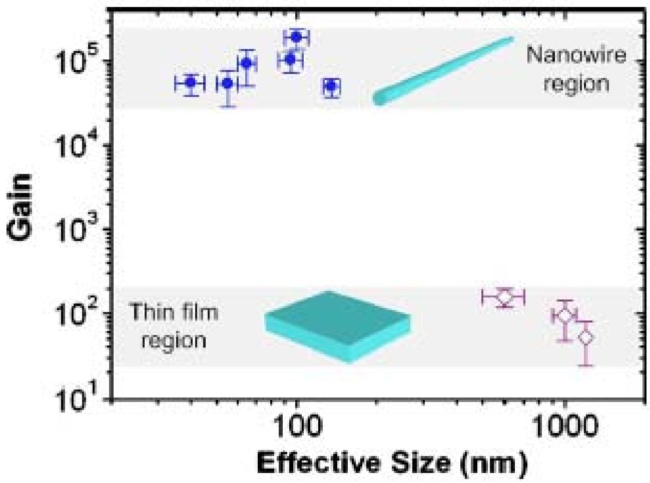

Figure 6 The photocurrent gain as a function of size for the GaN NWs (blue solid circles) and thin films (open purple diamonds) at 400 V/cm applied field and 4.0 eV excitation with 10–12 W/m^2 power density. The effective size is defined by the values of the NW diameter and the film thickness.

(4) Si nanotips: biomimetic nanostructures with broadband and quasi-omni-directional anti-reflection properties

Nanotips have attracted considerable interest in the last decade because of distinctive differences in their properties compared with bulk. Besides academic interest, nanotips also show promising potential for a variety of commercial applications, such as emitters in field emission display, nanometer-cantilevers, solar cells, and electrochemical electrodes. Nanotips arrays can be monolithic, i.e., formed from a single piece of material, as exemplified by selectively etching of a single substrate, where unetched portions of the substrate surface form the nanotips. Such monolithic approaches are attractive for easy integration with fabrication processes for semiconductor devices. There are numerous techniques for preparing nanotips, including, electron-beam lithography, condensing gas, depositing layer of varying thickness onto the substrate, or oxidizing portions of the substrate to form the nanomasks. The ECR process, having the ability to generate highest density of plasma of all, features a method for making nanotips arrays by forming masked and unmasked portions of the substrate, and simultaneously etching the unmasked portions of the substrate to form a plurality of nanotips resulting in an array.

The density of the nanomasks produced by ECR and thus nanotips can be higher than 10^{11} cm^{-2}. Of equal importance, these high-density nanotips can be produced by ECR uniformly over a large area, as demonstrated for a 6-inch Si wafer in Figure 7. Our patented process offers the opportunity to prepare high-density and well-aligned nanotips monolithically in one-step and is generally applicable to a wide range of materials [10].

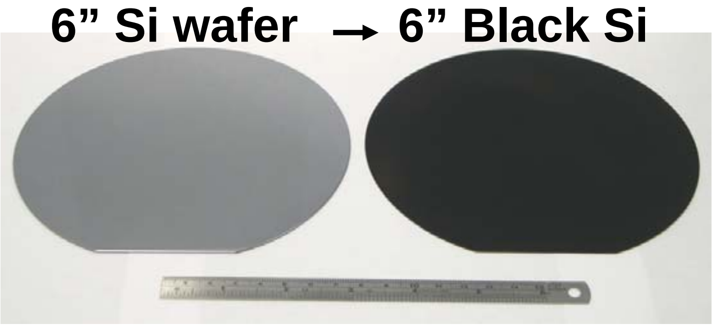

Figure 7 After ECR process an originally shinny silver-gray 6-inch Si wafer has been transformed to high-density arrayed SiNTs, which appears completely dark.

The large-area subwavelength structure of the arrayed Si nanotips wafer that mimicked a moth eye demonstrated a low hemispherical reflectance of <1% from UV to the IR region and show significant suppression of specular reflection in the far-IR to terahertz region (Figure 8). The specular reflection is nearly unaffected by varying the angle of incidence up to 70° of s- and p- polarized light [12]. A refractive index profile for the SiNT system can be generated using the gradient index of refraction approach, which in turn, can simulate the reflectance results as a function of incident angle for the s- and p-polarized light at wavelength 632.8nm. The remarkably high and featureless optical absorption in the aperiodic SiNTs, as against the periodic subwavelength structures, promises enhanced performance in solar cells.

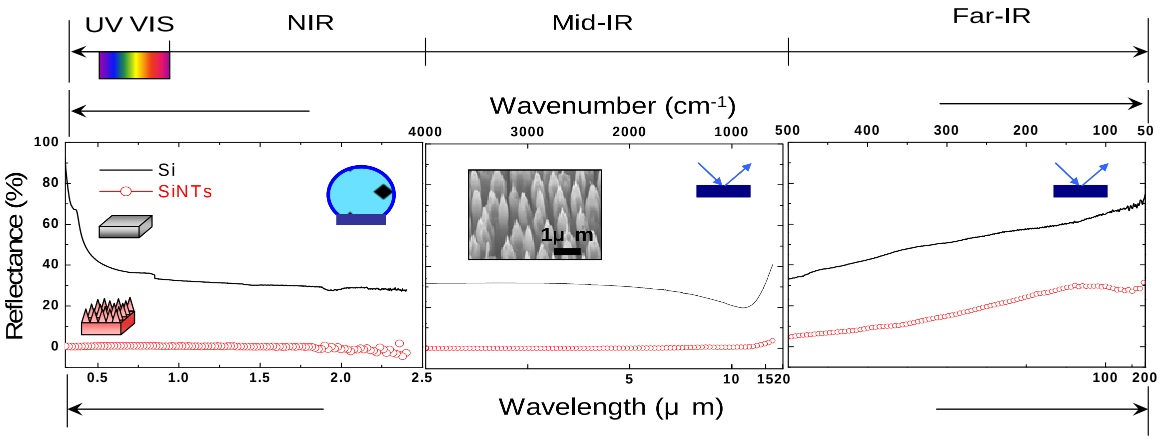

Figure 8 Broadband antireflection properties of SiNTs (-: Si wafer; □ : SiNTs)

(5) Polyaniline/Nafion composite membrane for direct methanol fuel cell operable at high methanol concentration with reduced methanol crossover

The DMFC, with the advantages of low temperature operation, ease of fuel storage and a simple design that requires no reformer, is regarded as a promising power source for portable electronic applications. However, commonly used proton-conducting layer such as Nafion 117 (N117) is highly permeable for methanol through the water-filled pores in the membrane, resulting in low fuel efficiency and reduced cathode activity due to the mixed potential effect and the mass-transfer effect at the cathode. Accordingly, a new proton-conducting membrane with low methanol permeability is essential to the development of DMFCs. In this study, protonated polyaniline (PANI) is directly polymerized on N117, forming a composite membrane (Figure 9), to act as a methanol-blocking layer to reduce the methanol crossover in the DMFC, which is beneficial for the DMFC operating at high methanol concentration.

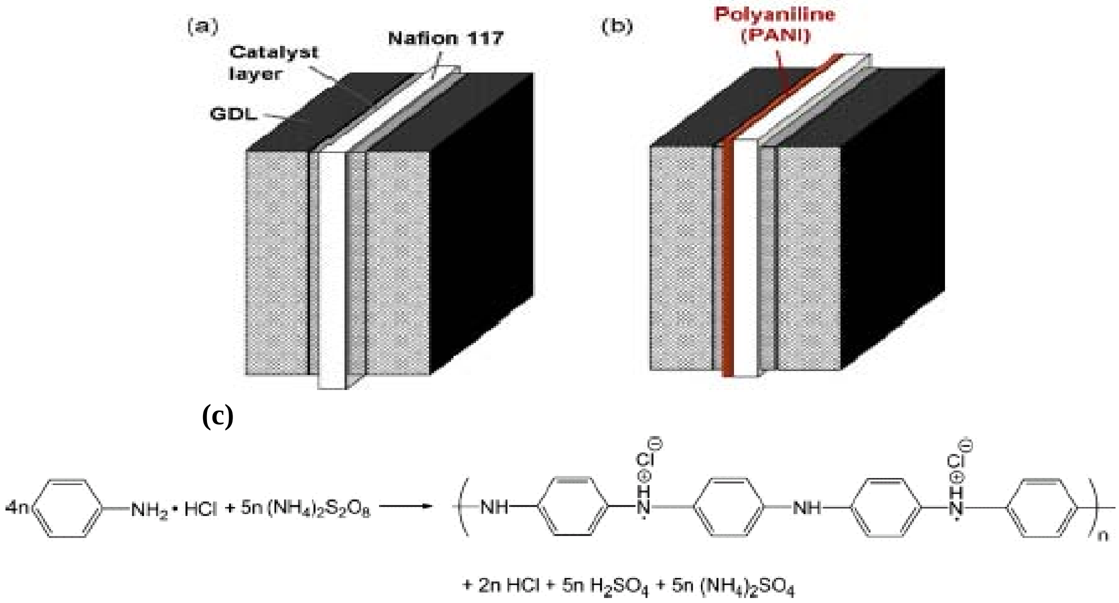

Figure 9 Schematic structures of the MEAs wherein (a) only the conventional Nafion 117 is used and (b) an extra methanol-blocking layer, polyaniline (PANI) is added to reduce the methanol crossover in the DMFC. (c) PANI is formed by oxidation of aniline hydrochloride with ammonium persulfate.

The PANI layer grown on the N117 with a thickness of 100 nm has an electrical conductivity of 13.2 S cm^{-1}. The methanol permeability of the PANI/N117 membrane is reduced to 59% of that of the N117 alone, suggesting that the PANI/N117 can effectively reduce the methanol crossover in the DMFC. Comparison of membrane-electrode-assemblies (MEA) using the conventional N117 and the newly developed PANI/N117 composite shows that the PANI/N117-based MEA outputs higher power at high methanol concentration, while the output power of the N117-based MEA is reduced at high methanol concentration due to the methanol crossover. The maximum power density of the PANI/N117-based MEA at 60 $^{\circ}$C is 70mWcm^{-2} at 6M methanol solution, which doubles the N117-based MEA at the same methanol concentration. The resistance of PANI/N117 composite membrane is reduced at elevated methanol concentration, due to the hydrogen bonding between methanol and PANI pushing the polymer chains apart. The fact that the PANI/N117-based MEA performs well at elevated methanol concentration suggests its suitability for the long-term operation of the DMFC.

(6) Enhanced charge separation by sieve-layer mediation in inorganic-organic solar cell

The biggest challenges facing the organic devices are the relatively poor charge transport and separation compared to their inorganic counterparts. In this study, we have introduced a new hybrid inorganic-organic photovoltaic (IN-OR PV) cell containing an interfacial layer, specifically, in the form of an electronic sieve layer that blocks hole diffusion and enhances charge separation and transport. Figure 10a shows a schematic of the IN-OR PV cell structure with a sieve layer incorporated and Figure 10b shows the ZnPc and Au layers with representative thicknesses. The sieve layer needs careful selection both in terms of its bandgap and its thickness. The electronic importance of the sieve layer can be visualized from the energy-band diagram shown in Figure 10c. A thin electronic sieve layer of LiF or SiO_x (x~0.4) was shown to increase the cell efficiency to 3.4 and 6.04%, respectively.

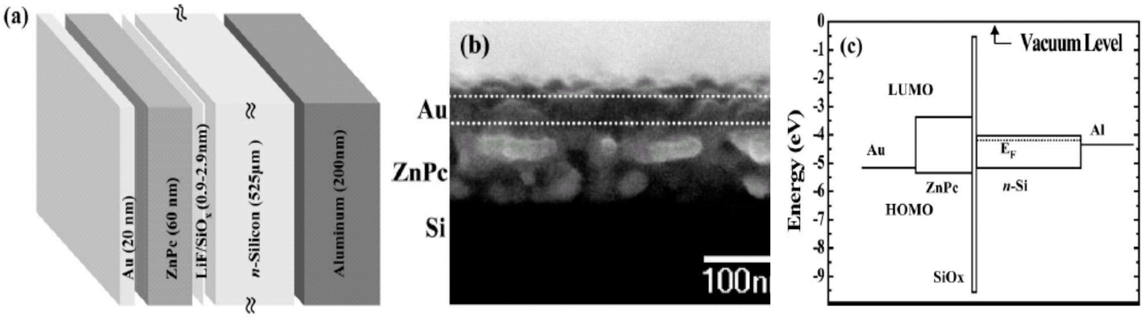

Figure 10 A schematic illustration of the cross section of the electronic-sieve-assisted IN-OR photovoltaic cell structure. b) A cross-sectional SEM image of the device showing the ZnPc and Au layers. c) The energy levels of the individual components of the photovoltaic cell.

It should be emphasized that control of both the composition and thickness of the oxide sieve layer is critical. The effect of the oxide layers prepared under different surface-current-induced-oxidation (SCIO) conditions on the cell performances is depicted in Figure 11.

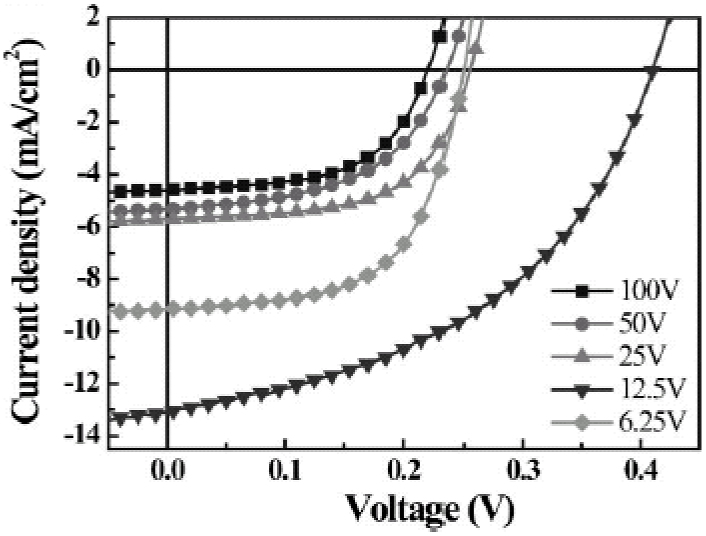

Figure 11 The current–voltage (J–V) characteristics of the photovoltaic devices with the oxide sieve layers prepared by surface-current-induced oxidation of silicon wafers at different current/voltage conditions.

Detailed analyses by scanning transmission electron microscopy (STEM) and electron-loss near-edge spectroscopy (ELNES) measurements (Tecnai G2 F20) are shown in Figure 12. Comparing the STEM image (Fig. 12a–b) and Si L2,3 ELNES (Fig. 12c–d) measurements performed on oxide layers produced at 12.5 V/1.1mA (yielding a power-conversion efficiency of 6.04%) and 100V/10mA (yielding a power-conversion efficiency of 1.44%), the difference in the nature and quality of the oxides is immediately evident. The oxide layer produced on Si at 100 V was SiO_x, with $1<x\sim2$, whereas that

produced at 12.5 V had SiO_x with $0.1<x<0.4$. This is pictorially depicted in the respective insets (Fig. 12a and b) as the variation of the ‘x’ value as a function of the depth of the scan. The thickness of both the oxide layers as measured by STEM (Fig. 12a–b) was between 2.7–3.5 nm. A purely Si-ZnPc interface would result in considerable hole diffusion towards the Al cathode (Fig. 10c), resulting in unwanted carrier recombination. A purely SiO_2-ZnPc interface, on the other hand, will hinder electron tunneling through the barrier, while nevertheless being a better hole-blocking layer. Our initial studies indicate an intermediate SiO_x, between Si and SiO_2, to be a more-effective sieve layer in performing the dual functions of hole blocking and efficient electron tunneling.

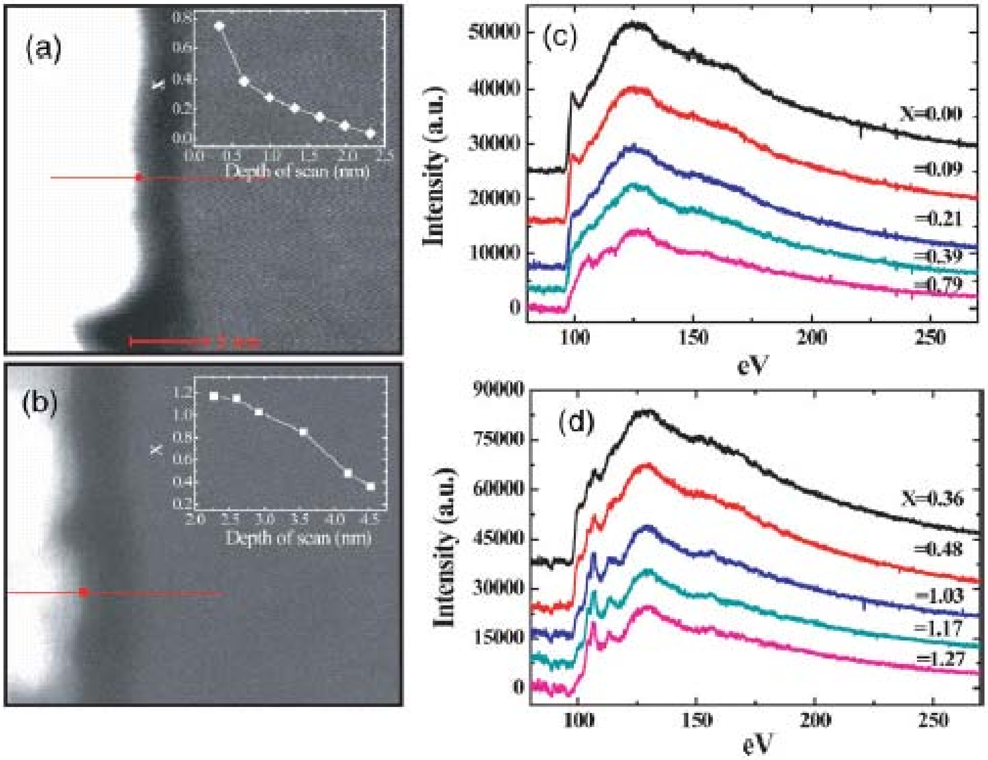

Figure 12 STEM image of the SiO_x layers produced at a) 12.5 V or 1.1 mA and b) 100 V or 10 mA. The scanning Si L2,3 ELNES measurements in (c) and (d) correspond to (a) and (b), respectively. The ‘x’ value for each Si L2,3 scan is shown on the plot. The insets in (a) and (b) show the marked distinction of the ‘x’ variation as a function of the depth of scan. The line of scan for the ELNES in both samples is shown. The scale bar for (a) and (b) is 5 nm.

Conclusion

An on-chip direct growth approach has been successfully applied to fabricate miniaturized micro-energy devices (such as direct methanol fuel cells and supercapacitors) as well as nano-optoelectronic and photovoltaic devices. The CNTs-based energy devices show high conductivity, efficient carrier collection and fast charge transfer kinetics. The GaN nanobridge devices exhibit an excellent visible-blind performance for the UV light detection and ultrahigh photocurrent generation efficiency. Meanwhile, the arrayed Si nanotips wafer that mimicked a moth eye demonstrated a low hemispherical reflectance of <1% from UV to the IR. The latter two results suggest high potential in both solar cell and defense applications. For organic-inorganic hybrids, interface control is crucial as exemplified in the roles of polyaniline nanowires as a methanol-blocking layer and LiF or SiO_x as a sieve layer to improve the stability and efficiency of the power devices.

References

[1] L. C. Chen, C. Y. Wen, C. H. Liang, W. K. Hong, K. J. Chen, H. C. Cheng, C. S. Shen, C. T. Wu and K. H. Chen, *Adv. Func. Mater. 12* (2002) 687.

[2] C. L. Sun, L. C. Chen, M. C. Su, L. S. Hong, O. Chyan, C. Y. Hsu, K. H. Chen, T. F. Chang and L. Chang, *Chem. of Mater. 17* (2005) 3749.

[3] Chia-Liang Sun, Houng-Wei Wang, Michitoshi Hayashi, Li-Chyong Chen and Kuei-Hsien Chen, *J. Am. Chem. Soc. 128* (2006) 8368.

[4] Chen-Hao Wang, Han-Chang Shih, Yu-Tai Tsai, He-Yun Du, Li-Chyong Chen, and Kuei-Hsien Chen, *Electrochimca Acta 52* (2006) 1612.

[5] C.-H. Wang, H.-Y. Du, Y.-T. Tsai, C.-P. Chen, C.-J. Huang, L. C. Chen, K. H. Chen, and H.-C. Shih, *J. Power Sources 171* (2007) 55.

[6] Wei-Chuan Fang, J. H. Huang, C. L. Sun, Li-Chyong Chen, Pagona Papakonstantinou, Oliver M. Chyan and Kuei-Hsien Chen, *J. Vac. Sci. Tech. B 24* (2006) 87.

[7] Wei-Chuan Fang, Kuei-Hsien Chen and Li-Chyong Chen, *Nanotechnology 18* (2007) Art. No. 485716.

[8] Wei-Chuan Fang, Min-Sheng Leu, Kuei-Hsien Chen and Li-Chyong Chen, *J. Electrochem. Soc. 155* (2008) K15.

[9] Reui-San Chen, Shiao-Wen Wang, Zon-Huang Lan, Jeff Tsung-Hui Tsai, Chien-Ting Wu, Li-Chyong Chen, Kuei-Hsien Chen, Y. S. Huang and C. C. Chen, *Small 4* (2008) 925.

[10] C. H. Hsu, C. F. Chen, H. C. Lo, D. Das, J. Tsai, J. S. Hwang, L. C. Chen and K. H. Chen, *Nano Lett. 4* (2004) 471.

[11] K. H. Chen, J. S. Hwang, H. C. Lo, D. Das and L. C. Chen, U. S. Patent 6,960,528 B2, Nov. 1 (2005).

[12] Yi-Fan Huang, Surojit Chattopadhyay, Yi-Jun Jen, Cheng-Yu Peng, Tze-An Liu, Yu-Kuei Hsu, Ci-Ling Pan, Hung-Chun Lo, Chih-Hsun Hsu, Yuan-Huei Chang, Chih-Shan Lee, Kuei-Hsien Chen, Li-Chyong Chen, *Nature Nanotech. 2* (2007) 770.

[13] Chien-Hong Lin, Surojit Chattopadhyay, Chia-Wen Hsu, Meng-Hsiu Wu, Wei-Chao Chen, Chien-Ting Wu, Shao-Chin Tsen, Jih-Shang Hwang, Jiun-Haw Lee, Cheng-Hsuan Chen, Li-Chyong Chen and Kuei-Hsien Chen, *Adv. Mater. 21* (2009) 759.

[14] Chen-Hao Wang, Chien-Chu Chen, Hsin-Cheng Hsu, He-Yun Du, Chin-Pei Chen, Jeong-Yuan Hwang, Li-Chyong Chen, Han-Chang Shih, Jaroslav Stejskal, Kuei-Hsien Chen, *J. Power Sources 190* (2009) 279.

[15] Ming-Hsien Hu, Wei-Ming Wang, Tzung Te Chen, Lu-Sheng Hong, Chun-Wei Chen, Chia-Chun Chen, Yang-Fang Chen, Kuei-Hsien Chen, and Li-Chyong Chen, *Adv. Func. Mater. 16* (2006) 537.

[16] Ming-Shien Hu, Geng-Ming Hsu, Kuei-Hsien Chen, Chia-Ju Yu, Hsu-Cheng Hsu, Li-Chyong Chen, Jih-Shang Hwang, Lu-Sheng Hong, and Yang-Fang Chen, *Appl. Phys. Lett. 90* (2007) 123109.

[17] Szu-Ping Fu, Chia-Ju Yu, T. T. Chen, Geng-Ming Hsu, Miin-Jang Chen, Li-Chyong Chen, Kuei-Hsien Chen, and Yang-Fang Chen, *Adv. Mater. 19* (2007) 4524.

[18] R. S. Chen, H. Y. Chen, C. Y. Lu, K. H. Chen, C. P. Chen, L. C. Chen, and Y. J. Yang, *Appl. Phys. Lett. 91* (2007) 223106.

Project Related Activities

During this work period, I have made a technical visit to AFRL Hanscom in March 31-April 1, 2008. My AFRL visit was arranged by Dr. Yu-Hui Chiu at Hanscom AFB. On the second day, Dr. Chiu has also brought us to meet Prof. Paulo C. Lozano, at the Department of Aeronautics and Astronautics, MIT. The opportunities of discussing the actual works pursued and needs at Hanscom AFRL and person-to-person discussion on the relevant technical issues are indeed valuable. Detail of this visit has been described in a separate WOS trip report. Frequent interaction with Dr. Yu-Hui Chiu has been continued till now. Joint efforts have also been exchanged. In fact, some CNTs specimens made in our lab were sent to Hanscom for testing and we have also received some tungsten wire/ribbon samples from Dr. Chiu for further nano-engineering and surface treatment. Preliminary results of our studies on tungsten have been sent to Dr. Chiu in a separate file.

Moreover, I have attended the annual AOARD-Taiwan Nano-workshop, both held in Hui-Sun Forest, Taiwan and San Francisco for 2008 and 2009, respectively. In fact, I have been to all of this series of workshops since the inauguration of the USAF-Taiwan Nano-initiatives (USAF/TNI) in 2004. Besides information exchange of the recent advancement in nanoscience and technology, such activities are valuable for the Taiwanese researchers to meet the researchers from the Air Force Research Laboratory (AFRL) as well as from other research institutes in the US. Some of the participants have either formed already or intended to form a team in the near future. After all the prior efforts and establishment, making a concerted effort to work collaboratively among the researchers from both sides on research topics relevant for the Air Force need is clearly intended in the most recent workshop. My main contact at AFRL, Dr. Yu-Hui Chiu and her collaborator, Prof. Paulo C. Lozano, Department of Aeronautics and Astronautics, MIT, have joined the 2009 workshop as well and presented their recent work on the nano-electrojet devices for space propulsion. Besides the emitter arrays based on Si lithographic technology, I also found the new emitter arrays based on porous tungsten emitter very interesting. Specifically, their initial tests on the wetting property of ionic liquid propellants appeared quite promising. During the workshop, we three have also extensively exchanged ideas and discussed potential topics for future collaboration. Some of the topics have already been included in our proposal recently submitted for the next fiscal year.

Appendix

I. Selective Project Related Publications

Overall, about 45 papers were published during this 2-yr project period. Financial support from AFOSR/AOARD has been indicated explicitly in the following 10 papers.

(1) 'Improved Broadband and Quasi-omni-directional Anti-reflection Properties with Biomimetic Silicon Nanostructure', Yi-Fan Huang, Surojit Chattopadhyay*, Yi-Jun Jen, Cheng-Yu Peng, Tze-An Liu, Yu-Kuei Hsu, Ci-Ling Pan, Hung-Chun Lo, Chih-Hsun Hsu, Yuan-Huei Chang, Chih-Shan Lee, Kuei-Hsien Chen, Li-Chyong Chen*, *Nature Nanotech. 2,* 770 (2007).

[This work was featured by *Asia-Materials*, a newly launched website by Nature Publishing Group, http://www.natureasia.com/asia-materials/highlight.php?id=68 and also highlighted on the website by Physics Research Promotion Center in Taiwan, http://prpc.phys.nthu.edu.tw/discovery.php.]

(2) 'Ultrahigh Photocurrent Gain in m-axial GaN Nanowires', R. S. Chen, H. Y. Chen, C. Y. Lu, K. H. Chen*, C. P. Chen, L. C. Chen*, and Y. J. Yang, *Appl. Phys. Lett. 91*, 223106 (2007).

(3) 'On-chip Fabrication of Well Aligned and Contact Barrier-Free GaN Nanobridge Devices with Ultrahigh Photocurrent Responsivity', Reui-San Chen, Shiao-Wen Wang, Zon-Huang Lan, Jeff Tsung-Hui Tsai, Chien-Ting Wu, Li-Chyong Chen*, Kuei-Hsien Chen*, Ying-Sheng Huang and Chia-Chun Chen, *Small 4,* 925 (2008).

(4) 'High-phase-purity Zinc-blende InN on R-plane Sapphire Substrate with Controlled Nitridation Pretreatment', Ching-Lien Hsiao, Ting-Wei Liu, Chien-Ting Wu, Hsu-Cheng Hsu, Geng-Min Hsu, Li-Chyong Chen*, Wen-Yu Hsiao, Chih-Chung Yang, Andreas Gällström, Per-Olof Holtz, Chia-Chun Chen and Kuei-Hsien Chen*, *Appl. Phys. Lett. 92*, 111914 (2008).

(5) 'Effects of Nitrogen-Doping on the Microstructure, Bonding and Electrochemical Activity of Carbon Nanotubes', Yan-Gu Lin, Yu-Kuei Hsu, Ju-Lan Yang, San-Yuan Chen, Kuei-Hsien Chen, and Li-Chyong Chen*, *Diamond & Relat. Mater. 18*, 433 (2009).

(6) 'Electrophoretic Deposition of PtRu Nanoparticles on Carbon Nanotubes for

Methanol Oxidation', Yu-Kuei Hsu, Ju-Lan Yang, Yan-Gu Lin, San-Yuan Chen, Li-Chyong Chen, and Kuei-Hsien Chen*, *Diamond & Relat. Mater. 18*, 557 (2009).

(7) 'Functionalized GaN Nanowires-based Electrode for Direct Label-free Voltammetric Detection of DNA Hybridization', Abhijit Ganguly, Chin-Pei Chen, Yao-Tong Lai, Chun-Chiang Kuo, Chih-Wei Hsu, Kuei-Hsien Chen* and Li-Chyong Chen*, *J. Mater. Chem. 19*, 928 (2009).

(8) 'Enhanced Charge Separation by Sieve-layer Mediation in High Efficiency Inorganic-organic Solar Cell', Chien-Hong Lin, Surojit Chattopadhyay, Chia-Wen Hsu, Meng-Hsiu Wu, Wei-Chao Chen, Chien-Ting Wu, Shao-Chin Tsen, Jih-Shang Hwang, Jiun-Haw Lee, Cheng-Hsuan Chen, Li-Chyong Chen*, and Kuei-Hsien Chen*, *Adv. Mater. 21*, 759 (2009).

(9) 'Low Methanol-Permeable Polyaniline/Nafion Composite Membrane for Direct Methanol Fuel Cell', Chen-Hao Wang, Chien-Chu Chen, Hsin-Cheng Hsu, He-Yun Du, Chin-Pei Chen, Jeong-Yuan Hwang, Li-Chyong Chen*, Han-Chang Shih, Jaroslav Stejskal, Kuei-Hsien Chen*, *J. Power Sources 190*, 279 (2009).

(10) 'Origin of the Anomalous Temperature Evolution of Photoluminescence Peak Energy in Degenerate InN Nanocolumns', P. C. Wei, S. Chattopadhyay*, F. S. Lin, C. M. Hsu, S. Jou, J. T. Chen, P. J. Huang, H. C. Hsu, H. C. Shih*, K. H. Chen, L. C. Chen*, *Optics Express 17*, 11690 (2009).

II. **Selective Project Related Invited Talks at International Conferences**

[AFOSR supports were explicitly acknowledged in the following invited presentations.]

(1) NanoSMAT (July 9-11, 2007), on *"Carbon nanotubes and related hybrids: towards integrated electrochemical energy micro-devices"*, Algarve, Portugal

(2) AVS-Second International Conference on One-dimensional Nanomaterials (ICON, September 26-29, 2007), on *"GaN nanowires for label-free bio-sensing applications"*, Malmö, Sweden

(3) 2008 MRS-Spring Meeting (March 24-28, 2008), Symposium P: Carbon Nanotubes and Related Low-dimensional Materials, on *"Carbon nanotubes for fuel cell and super capacitor applications"*, San Francisco, USA

(4) Second International Conference on New Diamond and Nano Carbons (NDNC, May 26-29, 2008), on *"Modification of CNTs for fuel cell and capacitor applications"*, Taipei, Taiwan

(5) 2008 MRS-International Materials Research Conference (IMRC, June 9-12, 2008), Symposium B: Sustainable Energy Materials, on *"Carbon nanotubes for fuel cell and super capacitor applications"*, Chongqing, China
[Highlighted at http://www.mrs.org/s_mrs/doc.asp?CID=14934&DID=212416#talks]

(6) AVS 55th International Symposium and Exhibition (Oct. 19-24, 2008), on *"Wafer-scale synthesis and electrochemical property of graphene formed by microwave plasma enhanced CVD"*, Boston, MA, USA

(7) 2008 MRS-Fall Meeting (December 1-5, 2008), Symposium TT: Local Structure and Dynamics in Amorphous Systems, on *"Multifunction nanoparticle-nanowire /nanotube composites: interface physics and chemistry"*, Boston, MA, USA

(8) SPIE-Photonics West (January 24-29, 2009), OE106: GaN Materials and Devices, on *"Photoconductivity, electrochemical and photoelectrochemical properties of GaN nanowires"*, & OE122: Materials, Devices and Applications for Solid State Lighting XIII, on *"Growth and luminescence properties of one-dimensional InN and InGaN nanowires"*, San Jose, CA, USA

(9) The First World Congress of International Academy of Nanomedicine, IANM 2009 (June 12-13, 2009), on "*High-sensitivity, label-free detection of DNA using GaN nanowire based electrode*", Hainan, China

(10) International Conference on Materials for Advanced Technologies ICMAT (June 28-July 3, 2009), Symposium H: Carbon Nanotubes: Syntheses, Characterization and Applications, on "*Wafer-scale synthesis and electrochemical properties of few-layer graphene for energy applications*", Singapore

III. Honors/Awards Received During This Project Period

III.1 Li-Chyong Chen

(1) Laureate of the Khwarizmi International Award, Iran (2009)

(2) International Federation of Inventors' Association Lady Prize (2009)

(3) Distinguished Visiting Research Fellowship, Royal Academy of Engineering, UK (2008)

(4) Distinguished Research Fellow, National Taiwan University, Taiwan (2007-)

(5) Honorary Doctor, Linköping University, Sweden (2007)

(6) Outstanding Research Award, National Science Council, Taiwan (2007)

III.2 Kuei-Hsien Chen

(1) Outstanding Scholar Awards of the Foundation for the Advancement of Outstanding Scholarship, Taiwan (2008-2013)

III.3 Our students/post-docs have won several best paper/poster awards in professional society national & international meetings in 2008, including the followings:

(1) Young Scientist Award, Best of Category and First Prize in the Chemistry Category, in Intel International Science and Engineering Fair (ISEF), Atlanta, USA (2008)

(2) Best Poster Award in Symposium on Sustainable Energy Materials, International Materials Research Conference (IMRC), Chongqing, China (2008)

(3) First Prize in MRS Fall 2008-Science as Art Contest, Boston (2008)